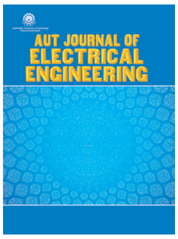

AUT Journal of Electrical Engineering

AUT J. Elec. Eng., 54 (Special Issue 2) (2022) 387-396
DOI: 10.22060/eej.2022.21167.5460

Transient Analysis of Donor-like Surface Traps in GaN HEMTs

A.A Chalechale[1], M. Shalchian[1*], F. Jazaeri[2]

[1] Electrical Engineering Department, Amirkabir University of Technology, Tehran, Iran.
[2]Researcher, Ecole Polytechnique Fédérale de Lausanne, Lausanne, Switzerland.

ABSTRACT: Charge trapping in Gallium Nitride based devices affect their reliability and performance. In this work we study the dynamics of charge capture and emission in donor-like surface traps and the impact of trapped charges on transient response of the drain current in Gallium Nitride High Electron Mobility Transistors (GaN HEMTs). To simulate transient characteristics, traps are excited into their empty or filled state by applying initial pulse on gate (gate-lag technique) or on drain (drain-lag) and then the drain current is monitored during transition toward steady state condition. The results show up to 44% variation in drain current level, which reflects the importance of trapped charges in the device characteristics. The effect of physical parameters, including trap energy level and temperature have been characterized using gate and drain-lag. A simple physical model is proposed (based on the Arrhenius relation) and calibrated with simulation results to obtain the emission and capture time-constants. The results extracted from the physical model show that the time constant for capture and emission varies from few microseconds up to few seconds depending on temperature and trap energy level and the result are in good agreement with TCAD simulations. This is an important step toward incorporation of charge trapping effect into the charge-based compact model of GaN HEMTs.

Review History:

Received: Feb. 28, 2022
Revised: Apr. 10, 2022
Accepted: Apr. 19, 2022
Available Online: Dec. 01, 2022

Keywords:

GaN HEMT
Trapping Effect
Current Collapse
Gate-lag
Drain-lag.

1- Introduction

AlGaN/GaN High Electron Mobility Transistors (HEMTs) are promising candidates for high-power and high-frequency applications due to their high breakdown voltages, high sheet carrier densities, and excellent performance at high temperatures due to high thermal conductivity of Gallium nitride [1-4]. However, dispersion effects induced from trapping phenomena, occurring in different locations of the device leads to critical issues and therefore can extremely limit the performance in such devices. Current collapse is one of the major dispersions originated from charge trapping effects, which has detrimental consequences on the device output characteristics [5-8]. In the recently developed charge-based EPFL HEMT model, the effect of charge trapping on device characteristics has not yet been included [2-4]. In the absence of charge trapping process, the dc and ac device characteristics predicted by the model have been validated against TCAD simulation results and experimental data. However, in order to accurately capture the characterization of the device performance, it is required to take the non-ideal charge trapping effects into consideration. In the presence of charge trapping, the conventional dc characteristics can no longer be representative of the device behavior at high frequencies. Therefore, pulsed characterization of the device, also known as pulsed-IV (a widely used technique), can be applied for such purposes [9]. Fig. 1 compares the TCAD simulation results obtained from dc voltage sweep (without the charge trapping effect), and pulsed-IV characteristics (with charge trapping effect). In this technique, the gate and drain voltages are pulsed from a quiescent bias point (V_{GSQ} = -6.8 V, V_{DSQ} = 10 V) to the final values of V_{GS} = -4 V to 0 V, V_{DS}=0 to 20 V. The pulsed I-V characteristics show significantly lower current level compared to DC measurements, which is the signature of trapped charges. Based on their location in the device structure, traps can be characterized into four groups: surface states, barrier traps, interface traps, and buffer/substrate traps [10-11]. Surface states and barrier traps are reported to be responsible for the gate-lag transient effect in GaN HEMTs, as shown in [12]. On the other hand, buffer layer traps or substrate traps are usually responded to drain voltage switching, and are therefore considered as the dominant cause of drain-lag related dispersion effects [13].

In this paper, the gate-lag and drain-lag turn-on techniques are employed to observe transient characteristics in the drain current when the gate and drain voltages are instantly pulsed within a short time domain. In this study, we have investigated the effects of traps located at the surface of the AlGaN layer since they have the highest impact on 2DEG charge density modulation [14]. These donor-like surface states lead to a delayed response in the drain current when the gate voltage is pulsed from an initial value below the pinch-off voltage to above turn-on voltage of the channel (Gate-lag) [8]. The delayed response of the current is due to a second puls-

---

*Corresponding author's email: shalchian@aut.ac.ir

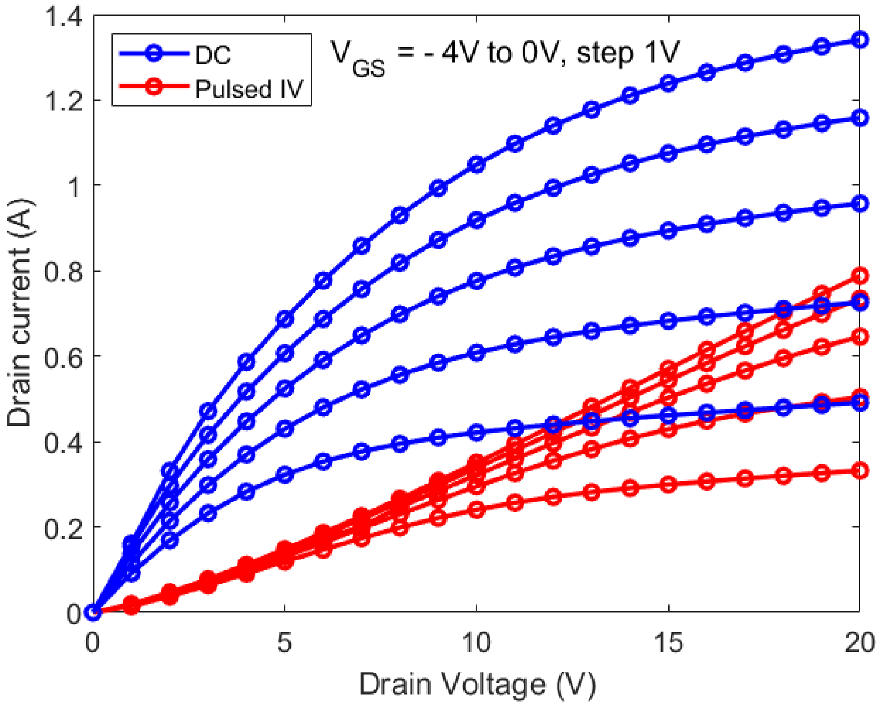

Fig. 1. Simulated ID-VD characteristics in the case of dc analysis (without traps) and pulsed-IV (with traps). The gate and drain voltages are pulsed from a quiescent bias point (VGSQ = -6.8 V, VDSQ = 10 V) to final values of V_{GS} = -4 V to 0 V, V_{DS}= 0 to 20 V

ing condition which allows the filling of the mentioned traps by electrons, and is similarly investigated (Drain-lag). The charge induced by these traps can modulate the free carrier density of the device by depleting the 2DEG density inside the GaN layer. The gate-lag effect has been experimentally studied by several other works [5, 6, 15, 16]. The aim of this paper is to study and characterize capture and emission time constants and relate those variables to physical parameters, including temperature and trap energy level. This result enables us to extend the charge-based compact model of GaN HEMT device to include the charge trapping effects.

This paper is organized as follows: in section 2, AlGaN/GaN HEMT structure, device parameters, models and assumptions used in numerical TCAD simulations are presented. In section 3, the gate-lag and drain-lag setups and simulation techniques are reviewed and simulation results are presented. In section 4, a physical model is used and calibrated to obtain the time constants of the emission and capture processes related to the gate-lag and drain-lag techniques, and the results are compared to TCAD simulations. Finally, section 5 concludes the paper.

2- Device Structure and Parameters

The AlGaN/GaN HEMT structure analyzed in this work is inspired from [17], and is shown in Fig. 2. The structure is used for both gate-lag and drain-lag techniques, and the physical parameters corresponding to each analysis is shown in Table 1. The two-dimensional device simulator used in this study is ATLAS, Silvaco [18]. The equation of Poisson and the continuity equations for electrons and holes are numerically solved, and the drift-diffusion transport model is used for the drain to source current derivation.

The spontaneous polarization and strain (piezoelectric effect) are considered as fixed sheet charges. A positive sheet charge +σpol = 1.5×1013 cm-2 was located at the interface of AlGaN/GaN. The equivalent negative sheet charge –σpol was located at the surface of AlGaN. Surface states included through a fixed donor trap density of σT1 = 4×1022 cm-3 (2x1015 cm-2) [17] and σT2 = 0.8×1020 cm-3 (4x1012 cm-2) respectively for gate-lag and drain-lag, are uniformly distributed on the ungated surface between the electrodes and with a depth of 5 A° within the AlGaN layer. We have used k.p model in our simulation to take into account the quantum confinement in the quantum well formed in the surface of the GaN part of AlGaN/GaN layer [18]. The dynamic traps are simulated by a Shockley-Read-Hall recombination term, included in the continuity equations. An additional differential rate equation is solved to account for the capture and emission processes in the transient trap simulations. The capture cross sections considered for electrons and holes (σn = σp) are consistent with the values of other reported numerical simulations [17, 19, 20]. The discrete trap energy level with reference to the top of the valance band is considered as a parameter in this study. Table 2 shows the values for doping and mobility used in TCAD simulations.

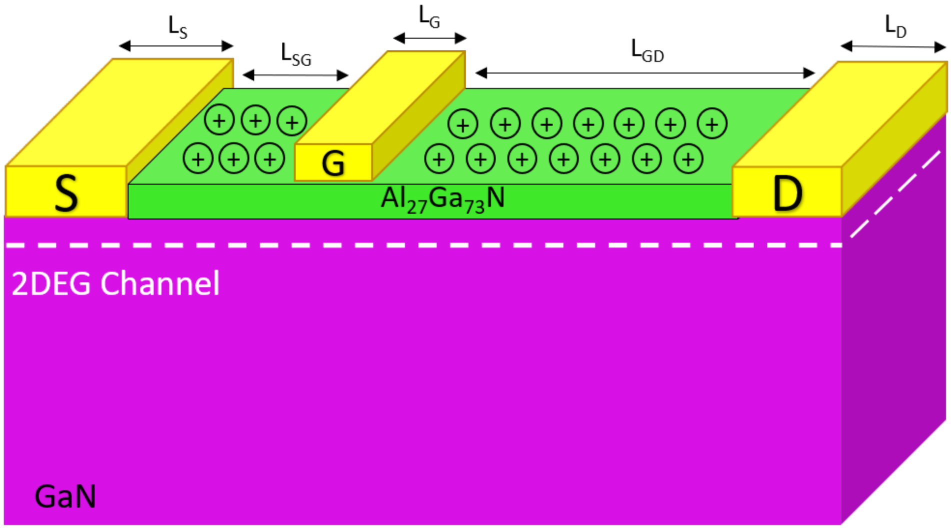

Fig. 2. 3-D schematic cross section of the simulated AlGaN/GaN HEMT device in the presence of donor-like surface traps (⊕ symbols)

Table 1. Physical parameters for gate-lag and drain-lag analysis used in TCAD simulations

Parameter	Value (gate-lag) [17]	Value (drain-lag) [20]
Al composition	27 %	36 %
AlGaN thickness	30 nm	20 nm
GaN thickness	2.97 µm	0.9 µm
Gate length (L_G)	0.6 µm	5 µm
Source-gate length (L_{SG})	0.9 µm	1.5 µm
Drain-gate length (L_{DG})	1.5 µm	2 µm
Electron and hole capture cross sections ($\sigma_n = \sigma_p$)	1×10^{-15} cm^2	1×10^{-19} cm^2

Table 2. Values of doping and mobility used in TCAD simulations (gate-lag and drain-lag)

Parameter	Value
Source & Drain doping	5×10^{18} cm^{-3}
Electron mobility in AlGaN	100 cm^{2}V^{-1}s^{-1}
Hole mobility in AlGaN	5 cm^{2}V^{-1}s^{-1}
Electron mobility in GaN	1100 cm^{2}V-^{1}s^{-1}
Hole mobility in GaN	30 cm^{2}V^{-1}s^{-1}

3- Simulation Method and Results

The gate-lag turn-on technique is utilizable by applying a transient voltage step to the gate terminal, while keeping the drain voltage at a constant value. Fig. 3 (a) shows the circuit setup and biasing protocol used for this technique implemented in our transient simulations, and also the corresponding effect on the position of the surface states within the band diagram. A fixed voltage of 10 V is applied to the drain terminal, and the gate terminal is pulsed from the quiescent bias point of an off-state value below pinch-off (V_{GS} = – 10 V) to a turn-on potential (V_{GS} = 0 V). The transient device current ($I_D(t)$) is simulated under these conditions for 20 s to observe the emission process. The emission time from the trap depends on the trap energy level, and we used the transient time of 20 seconds to observe the contribution of various traps with different energies. To associate the circuit represented in Fig. 3 (a) to the simulated device of Fig. 1, a Mixed-mode TCAD simulator has been used [18], which integrates circuit and device simulators and allows us to merge both as a SPICE-like netlist. Fig 3 (c) shows the charge state of traps for two excitation states of "0" and "1" applied by Vgs, respectively. Positive voltage discharges the trap after a characteristic time called the emission time, and the results in this step increase in 2-DEG charge density and current level.

Fig. 4 shows the transient drain current in response to the pulsed gate voltage for different values of donor trap energy levels. The energy level E_T is measured referenced to the top of the valence band. The reference curve shows the transient response for the device without any trapping process. Fig.4 also compares the results of this study to the results presented in [17], which shows very similar characteristics. The simulations have been performed at room temperature (T = 300 K). A donor-like trap can be either positive or neutral, similar to a donor dopant. A donor-like trap is positively charged (ionized) when is empty and neutral when is filled with an electron [21]. Two major effects can be noticed in the current characteristics of Fig. 4. The first effect is a transient step in the current level, which is lower than the final current level (in the order of 0.5 A/mm to 0.7 A/mm), followed by a current jump to its final value in the order of 1.1 A/mm to 1.25 A/mm. The transient step is the result of current collapse phenomenon. This can be attributed to the formation of a virtual gate next to the gate contact [8]. In other words, the surface donor states located in the ungated surface between the contacts can capture the electrons injected from the gate through tunneling mechanisms during the pre-pulse condition. presently, the channel is not solely controlled by the gate terminal, but these trapped electrons also contribute in controlling the channel underneath by partially depleting the 2DEG and acting as a secondary gate next to the main gate contact. The amount of the transient drain current reduction obtained from Fig. 4 with respect to the reference curve is almost 44%, which is analogous to the experimentally obtained values (~40%) for a drain bias value of V_{DS} = 10 V [8].

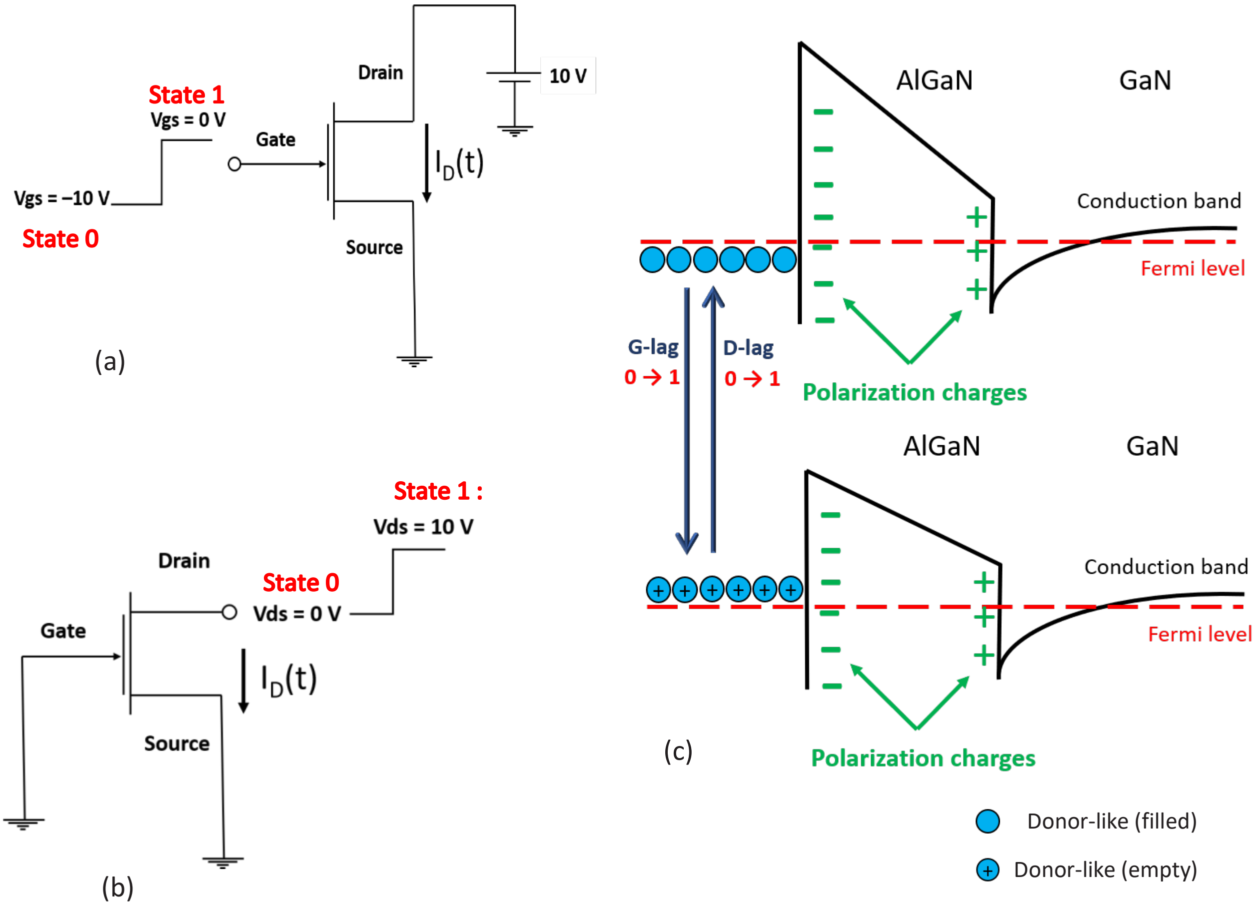

Fig. 3. Circuit setup used to implement transient gate-lag and drain-lag turn on techniques. (a) gate-lag technique setup. (b) drain-lag technique setup. (c) band diagrams showing the trap states in both cases (gate-lag and drain-lag).

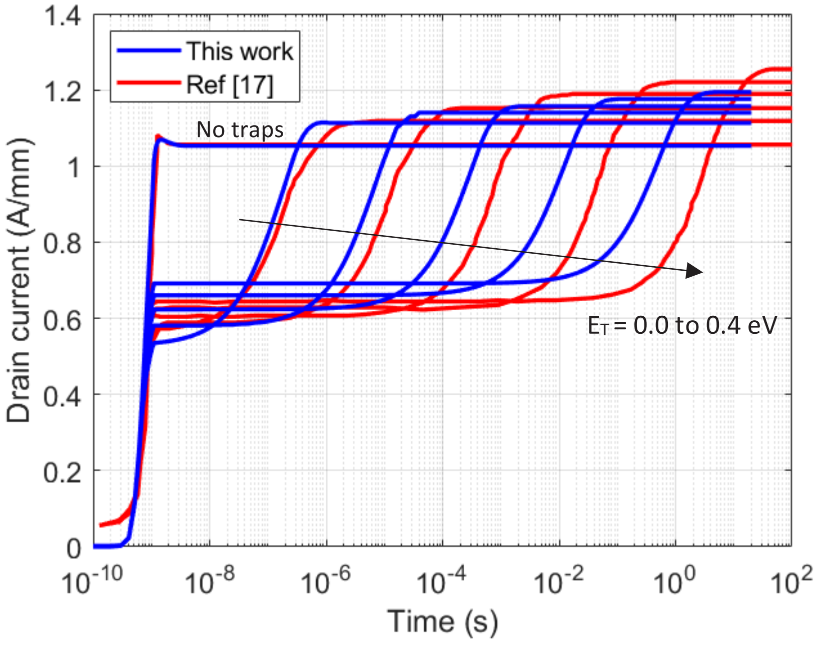

Fig. 4. Simulated drain current gate-lag transient characteristics for the case of: (I) no traps, and (II) donor trap energy levels of ET = 0.0, 0.1, 0.2, 0.3 and 0.4 eV. blue lines: TCAD simulations, red lines: results from [17].

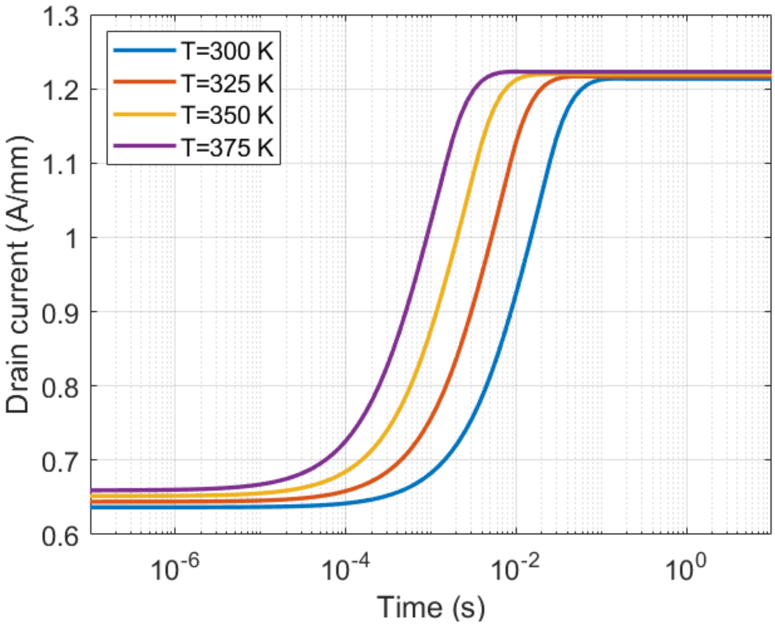

Fig. 5. Simulated drain current transient gate-lag characteristics under different temperatures. T = 300, 325, 350 and 375 K. (ET = 0.3 eV)

The second effect observed in the transient characteristics of Fig. 4, is an increase of the duration of the transient step, which is linked to emission time constants as the energy levels increase from 0.0 to 0.4 eV above the valence band. This parameter varies from nanoseconds for trap energy level of 0.0 eV to seconds for a trap level of 0.4 eV as extracted from Fig. 4 (the horizontal axis is in logarithmic scale). Similar time constants have been reported for surface traps emission in AlGaN/GaN HEMTs [6, 22, 23]. In addition, temperature variation has a huge role in the trapping and de-trapping processes [24]. Fig. 5 shows the current gate-lag transient characteristics obtained at different temperatures for trap energy level of E_T = 0.3 eV. As can be seen, increasing the temperature results in faster emission rate. In other words, it would be easier for the charges to de-trap at higher temperatures. We may use a simple physical model to relate the transient characteristics with the temperature and trap energy levels. This model is discussed in the following section.

Fig. 6 shows the TCAD transient simulations of drain-lag and gate-lag turn-on technique at room temperature (T = 300 K). In both techniques, the current finally settles down to the same value after a transient period, however in the drain-lag technique, the current level is high at the beginning and gradually decreases toward the final value. This can be explained by considering that a large number of traps are initially depleted from electron charges in the pre-pulsed condition and some of them would capture electrons and reach the steady state condition. This means that, positive voltage on the secondary gate decreases with time due to the filling of the traps and finally reaches a steady state value. As clearly shown in fig. 6, as the energy level of trap increases, it taes longer time to reach the steady state current level which means the capture time increases.

Fig. 7 shows the capture process of a trap energy level of E = 0.3 eV at various temperatures. Faster capture times are observed in higher temperatures, a behavior analogous to gate-lag related emission time constants.

We have also compared the simulation results with the experimental and simulation results presented in [20] using similar physical parameters as listed in Table. 1, column (II). Fig. 8 shows comparison for ET=0.25 eV, indicating very good agreement between the simulation and experimental data except for a short transient time at the beginning. This result confirms validity of the interface trap model and drain-lag characterization protocol used in TCAD simulation.

4- Physical Model for Time Constants

From a physical point of view, the transition from "full" to "empty" state is a stochastical process, described as a Markov process [25]. The probability of transition as a function of time is obtained from the Master equation, which is a first order differential equation in time domain and shows exponential decay characteristics with a time constant, called emission time constant.

The emission time constant ($t_{emission}$) is related to the trap energy level depicted in Fig. 4. We may extract the emission time constant from simulation results by measuring the time difference between the initial drain current peak value and the point in the middle of falling transition step, as in Eq. (1).

$$\tau_{emission} = t_{\left(\frac{I_{initial} + I_{final}}{2}\right)} - t_{(I_{initial})} \qquad (1)$$

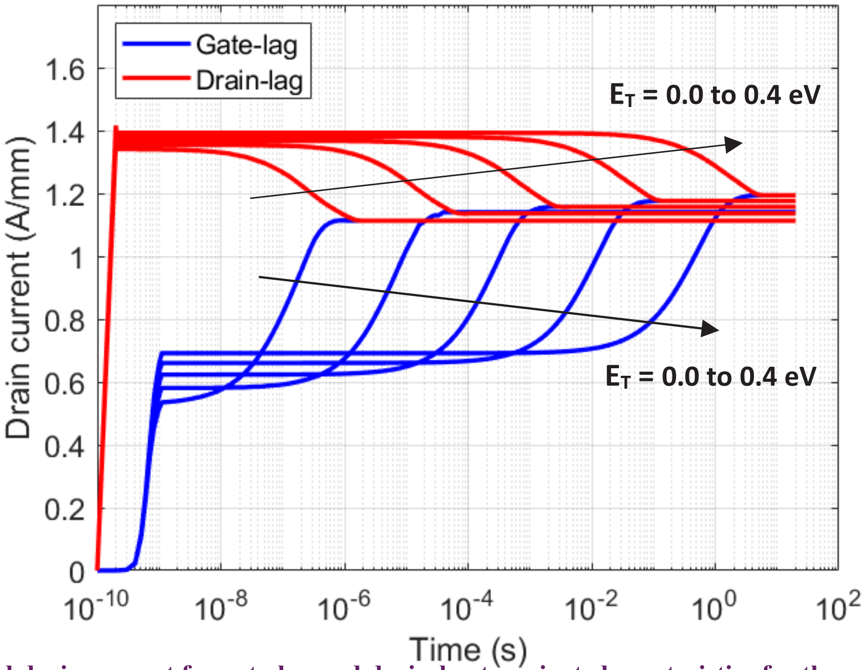

Fig. 6. Simulated drain current for gate-lag and drain-lag transient characteristics for the case of donor trap energy levels of ET = 0, 0.1, 0.2, 0.3 and 0.4 eV.

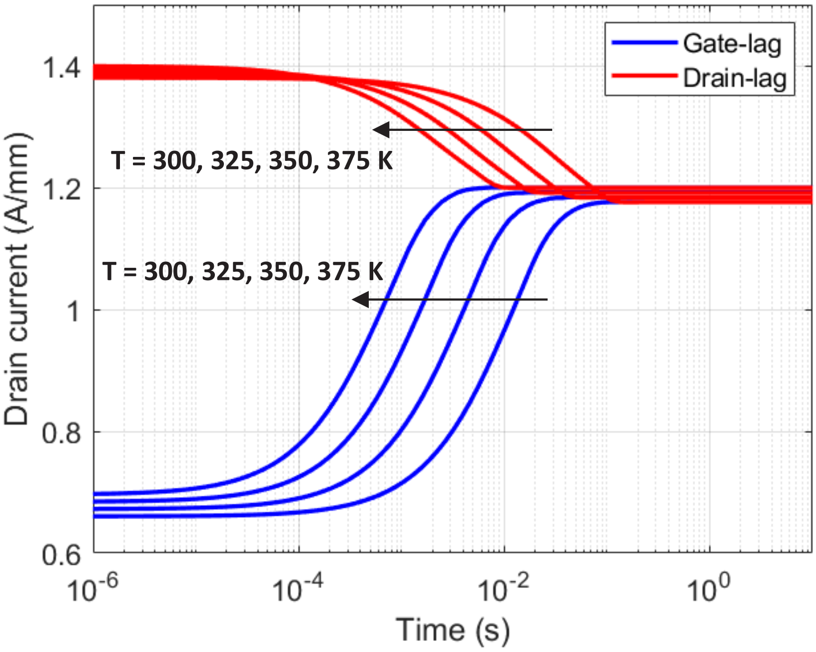

Fig. 7. Simulated drain current transient for gate-lag and drain-lag characteristics under different temperatures. T = 300, 325, 350 and 375 K. (ET = 0.3 eV)

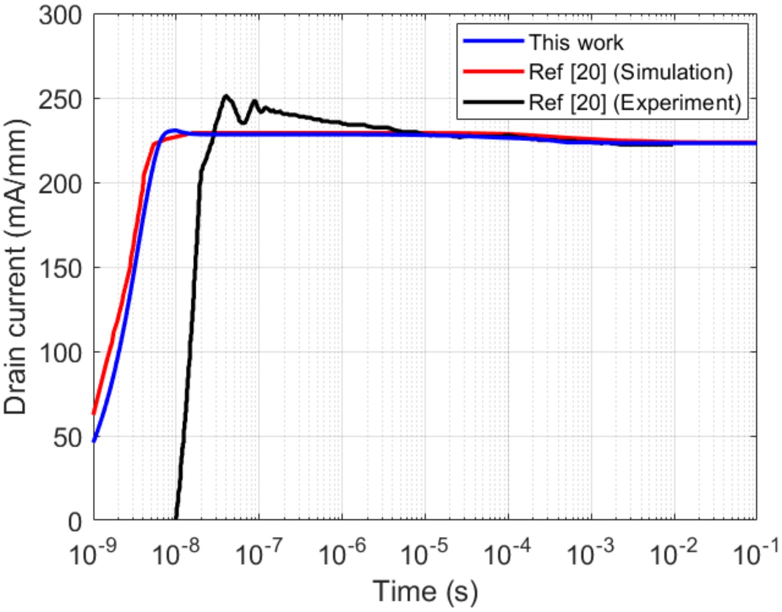

Fig. 8. Simulated drain current transient (drain-lag) characteristics compared with the results of [20].

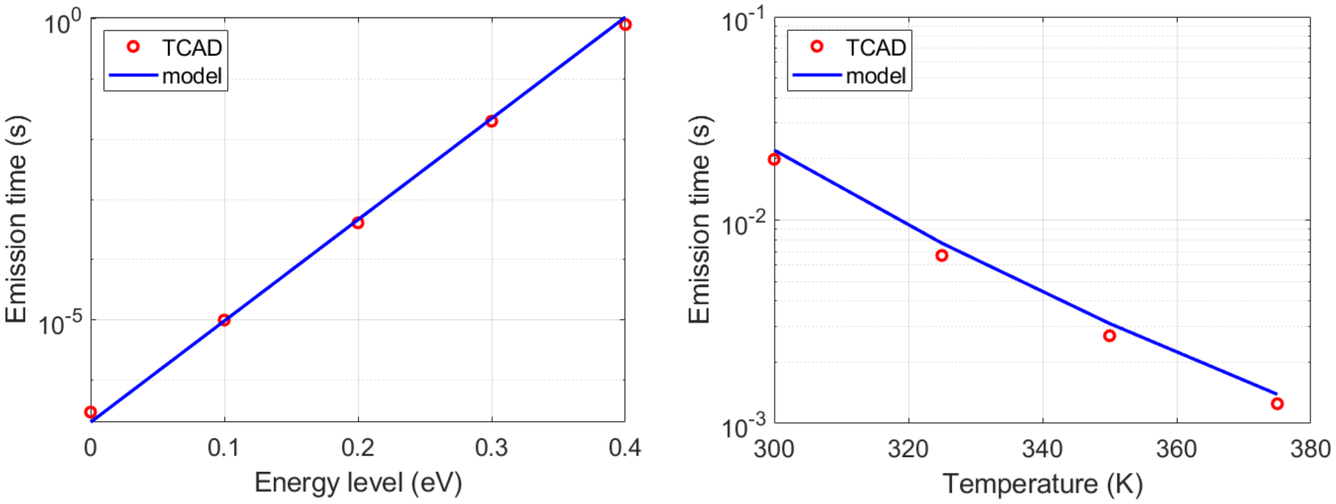

Fig. 9. Comparison of emission time constants obtained from TCAD and model with respect to trap energy levels at T=300 K (a) and with respect to temperature for a trap level of ET = 0.3 eV (b). y-axis is set to log10 scale.

where $I_{initial}$ and I_{final} are the values of the drain current at the initial turn-on step and at the end of the emission process, respectively. Fig 9 shows emission time constant as a function of trap energy extracted from TCAD transient simulations in the logarithmic scale. The emission rate of an electron from a trap level can be obtained from the Arrhenius relation given below [12].

$$e_n = AT^2 \, exp\left[-\frac{E_A}{kT}\right] \qquad (2)$$

where e_n[1/s] is the trap emission rate, T is the temperature, k is the Boltzmann constant, E_A is the activation energy of the trapped charge and A is a constant which is proportional to the trap capture cross section [12]. By choosing an appropriate value for A (170 [1/ s.K^2]) as a fitting parameter in Eq. (2), one can reproduce the time constants of the emission process with respect to variations of two main physical parameters, i.e., the energy level and the temperature. (a), compares the time constants obtained from Eq. (2), with the values extracted from Fig. 3 for five different energy levels at T = 300 K. Fig. 9 (b) also manifests the agreement between

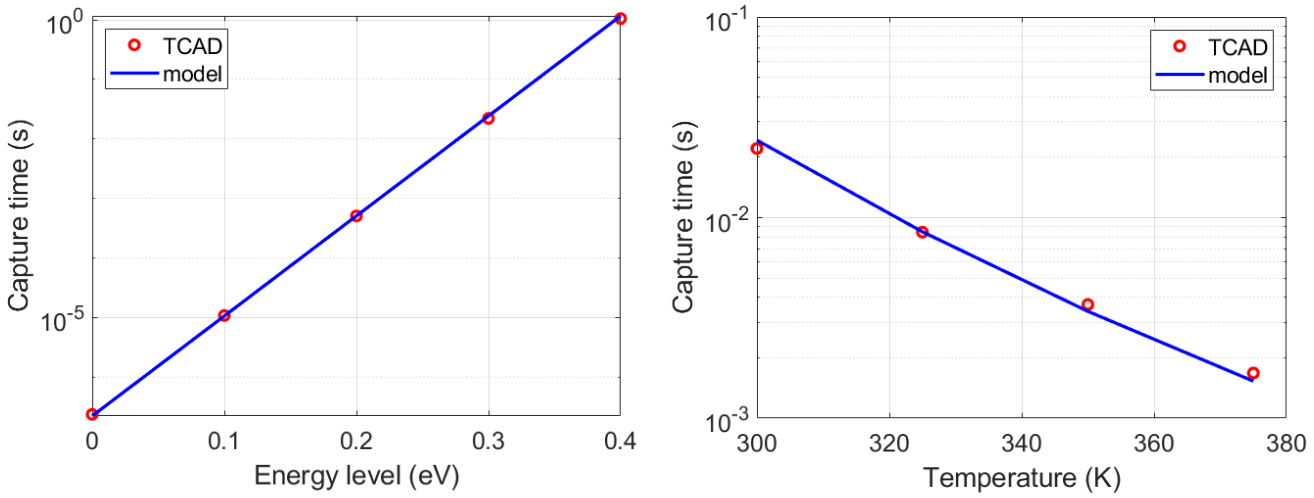

Fig. 10. Comparison of capture time constants obtained from TCAD and model with respect to trap energy levels at T=300 K (a) and with respect to temperature for a trap level of ET = 0.3 eV (b). y-axis is set to log10 scale.

model and TCAD simulations in time constants for a constant energy level of $E_T = 0.3$ eV, and at several temperatures in the range of 300 K to 380 K.

To extract the capture time constants corresponding to the trap energy level from TCAD simulation results of Fig. 7, we used Eq. (1), similar to emission time constant extraction. The rate of electron capture inside a trap in a filling process is affected by the trap's capture cross section parameter. As mentioned in the previous section, the calibration parameter A is used to account for this dependency. Thus, by changing A in Eq. (2), it is possible to reintroduce a similar physical model for the capture time constant which is in agreement with TCAD simulation results (A=60 [1/ s.K^2]). Fig. 10 (a) compares the time constants related to the capture of electrons in the drain-lag technique extracted from TCAD simulations of Fig. 7 and the model. Fig. 10 (b) also shows agreement between the extracted values of TCAD and model for a constant trap energy level of ET = 0.3 eV in four different temperatures.

5- Conclusion

In this paper, the impact of donor-like traps on the transient characteristics of the device triggered by a gate-lag and drain-lag turn-on techniques are investigated through TCAD simulations. We assumed that the transient response of traps follows the master equation with the exponential decay response and a time constant based on Arrhenius relation. This physical picture is used to characterize the effects of trap activation energy and temperature on the transient characteristics of both methods. The trap emission times obtained from physical model are found to be consistent with the extracted values from TCAD simulation, and also reported from measurements [6, 22, 23]. The results of this study are physically sound and can be used for compact modelling of the device characteristics. Further investigation is ongoing to study the effects of other types of traps on the characteristics of AlGaN/GaN HEMTs.

List of symbols

A	constant parameter, 1/ s.K^2
E_A (E_T)	Trap activation energy, eV
e_n	emission rate, 1/s
$I_{initial}$	Drain current at transient step, A/mm
I_{final}	Drain current at end of emission(capture), A/mm
k	Boltzmann constant, eV/K
L_G	Gate length, µm
L_{SG}	Source-gate length, µm
L_{DG}	Drain-gate length, µm
T	temperature, K
σ_n	Electron capture cross section, cm^2
σ_p	Hole capture cross section, cm^2
σ_{pol}	Polarization charge, cm^{-2}
σ_T	Donor trap density, cm^{-3}
$\tau_{emission}$	Emission time from trap, s

References

[1] U.K. Mishra, P. Parikh, Y.-F. Wu, "AlGaN/GaN HEMTs-an overview of device operation and applications," Proceedings of the IEEE, 90(6) (2002) 1022-1031.

[2] F. Jazaeri, J.-M. Sallese, "Charge-based EPFL HEMT model," IEEE Transactions on Electron Devices, 66(3) (2019) 1218-1229.

[3] F. Jazaeri, M. Shalchian, J.-M. Sallese, Transcapacitances in EPFL HEMT model, IEEE Transactions on Electron Devices, 67(2) (2019) 758-762.

[4] M. Allaei, M. Shalchian, F. Jazaeri, Modeling of short-channel effects in GaN HEMTs, IEEE Transactions on Electron Devices, 67(8) (2020) 3088-3094.

[5] S. Trassaert, B. Boudart, C. Gaquiere, D. Theron, Y. Crosnier, F. Huet, M. Poisson, Trap effects studies in GaN MESFETs by pulsed measurements, Electronics Letters, 35(16) (1999) 1386-1388.

[6] I. Daumiller, D. Theron, C. Gaquiere, A. Vescan, R. Dietrich, A. Wieszt, H. Leier, R. Vetury, U. Mishra, I. Smorchkova, Current instabilities in GaN-based devices, IEEE Electron Device Letters, 22(2) (2001) 62-64.

[7] S.C. Binari, K. Ikossi, J.A. Roussos, W. Kruppa, D. Park, H.B. Dietrich, D.D. Koleske, A.E. Wickenden, R.L. Henry, Trapping effects and microwave power performance in AlGaN/GaN HEMTs, IEEE Transactions on Electron Devices, 48(3) (2001) 465-471.

[8] R. Vetury, N.Q. Zhang, S. Keller, U.K. Mishra, The impact of surface states on the DC and RF characteristics of AlGaN/GaN HFETs, IEEE Transactions on Electron Devices, 48(3) (2001) 560-566.

[9] M. Meneghini, C. De Santi, T. Ueda, T. Tanaka, D. Ueda, E. Zanoni, G. Meneghesso, Time-and field-dependent trapping in GaN-based enhancement-mode transistors with p-gate, IEEE Electron device letters, 33(3) (2012) 375-377.

[10] B. Syamal, X. Zhou, S.B. Chiah, A.M. Jesudas, S. Arulkumaran, G.I. Ng, A comprehensive compact model for GaN HEMTs, including quasi-steady-state and transient trap-charge effects, IEEE Transactions on Electron Devices, 63(4) (2016) 1478-1485.

[11] J. Grisolia, M. Shalchian, G.B. Assayag, H. Coffin, C. Bonafos, S. Schamm, S. Atarodi, A. Claverie, The effects of oxidation conditions on structural and electrical properties of silicon nanoparticles obtained by ultra-low-energy ion implantation, Nanotechnology, 16(12) (2005) 2987.

[12] O. Mitrofanov, M. Manfra, Mechanisms of gate lag in GaN/AlGaN/GaN High Electron Mobility Transistors, Superlattices and Microstructures, 34(1-2) (2003) 33-53.

[13] G. Meneghesso, G. Verzellesi, F. Danesin, F. Rampazzo, F. Zanon, A. Tazzoli, M. Meneghini, E. Zanoni, Reliability of GaN high-electron-mobility transistors: State of the art and perspectives, IEEE Transactions on Device and Materials Reliability, 8(2) (2008) 332-343.

[14] J.P. Ibbetson, P. Fini, K. Ness, S. DenBaars, J. Speck, U. Mishra, Polarization effects, surface states, and the source of electrons in AlGaN/GaN heterostructure field effect transistors, Applied Physics Letters, 77(2) (2000) 250-252.

[15] S. Binari, W. Kruppa, H. Dietrich, G. Kelner, A. Wickenden, J. Freitas Jr, Fabrication and characterization of GaN FETs, Solid-State Electronics, 41(10) (1997) 1549-1554.

[16] G. Meneghesso, A. Chini, E. Zanoni, M. Manfredi, M. Pavesi, B. Boudart, C. Gaquiere, Diagnosis of trapping phenomena in GaN MESFETs, in: International Electron Devices Meeting 2000. Technical Digest. IEDM (Cat. No. 00CH37138), IEEE, 2000, pp. 389-392.

[17] J. Tirado, J. Sanchez-Rojas, J. Izpura, Simulation of surface state effects in the transient response of AlGaN/GaN HEMT and GaN MESFET devices, Semiconductor science and technology, 21(8) (2006) 1150.

[18] I. Silvaco, ATLAS user's manual device simulation software, Santa Clara, CA, (2010).

[19] C. Miccoli, V.C. Martino, S. Reina, S. Rinaudo, Trapping and thermal effects analysis for AlGaN/GaN HEMTs by means of TCAD simulations, IEEE Electron Device Letters, 34(9) (2013) 1121-1123.

[20] J.M. Tirado, J.L. Sanchez-Rojas, J.I. Izpura, Trapping effects in the transient response of AlGaN/GaN HEMT devices, IEEE Transactions on Electron Devices, 54(3) (2007) 410-417.

[21] F. Jazaeri, C.-M. Zhang, A. Pezzotta, C. Enz, Charge-based modeling of radiation damage in symmetric double-gate MOSFETs, IEEE Journal of the Electron Devices Society, 6 (2017) 85-94.

[22] S.C. Binari, P. Klein, T.E. Kazior, Trapping effects in GaN and SiC microwave FETs, Proceedings of the IEEE, 90(6) (2002) 1048-1058.

[23] G. Meneghesso, G. Verzellesi, R. Pierobon, F. Rampazzo, A. Chini, U.K. Mishra, C. Canali, E. Zanoni, Surface-related drain current dispersion effects in AlGaN-GaN HEMTs, IEEE Transactions on Electron Devices, 51(10) (2004) 1554-1561.

[24] S. Mase, A. Wakejima, T. Egawa, Analysis of carrier trapping and emission in AlGaN/GaN HEMT with bias-controllable field plate, physica status solidi (a), 214(8) (2017) 1600840.

[25] T. Grasser, Stochastic charge trapping in oxides: From random telegraph noise to bias temperature instabilities, Microelectronics Reliability, 52(1) (2012) 39-70.

HOW TO CITE THIS ARTICLE

A.A Chalechale, M. Shalchian, F. Jazaeri, Transient Analysis of Donor-like Surface Traps in GaN HEMTs. AUT J. Elec. Eng., 54(Special Issue 2) (2022) 387-396.

DOI: 10.22060/eej.2022.21167.5460